



Technical Report

Automated Data Collection for Modelling Texas Instruments Ultra Low-Power Chargers

Mojtaba Masoudinejad

7/2017



Part of the work on this technical report has been supported by Deutsche Forschungsgemeinschaft (DFG) within the Collaborative Research Center SFB 876 "Providing Information by Resource-Constrained Analysis", project A4.

Speaker: Prof. Dr. Katharina Morik
Address: TU Dortmund University
Joseph-von-Fraunhofer-Str. 23
D-44227 Dortmund
Web: <http://sfb876.tu-dortmund.de>

1 Introduction

Cyber Physical Systems (CPS) are changing the face of future computing. Forthcoming systems are mostly mobile and have a different perspective compared to the stationary solutions. During the last decade, number of these smart devices has been increasing rapidly [1]. Consequently, complex decision making processes are replaced by many non-stationary objects. These systems are available in a wide span of contexts. From sensing modules, computing and even smart actuation devices [2]. In spite of specific name within each field, the term *entity* is commonly used as a general concept for these objects.

A key advantage of these smart entities is the flexibility of the overall system structure. Each device works as an individual entity while it can cooperate with local environment and other entities. This makes systems with multiple cooperative schemes possible, leading to the highest structure flexibility. Entities can be added or removed from a system at each instant while the rest continue operating. This flexibility and modularity is what many applications such as materials flow and logistics had always demanded [3, 4] .

Cooperation of entities requires communication in between them. This aspect has been playing a critical role for developments during last few years. Its main expression is the communication role in accordance to the Internet of Things (IoT) revolution. Accordingly, research on communication systems specially in the wireless form has gained momentum.

Many researches in this field promise better throughput, larger communication distances and higher quality of service. However, energy demand of these systems is still a challenging aspect for developing many CPS entities. Researches such as [5, 6] had shown that the energy demand for wireless communication is much larger than the rest of the energy demands in a CPS device. Although availability of ultra low-power components made the overall IoT revolution possible, energy concerns are still available. Also, the always growing need for communicating more often, higher data rates and longer telegram length intensifies this quest.

A traditional systems with a battery assures an acceptable life cycle for an entity. However, increase in the communication demand in addition to the growing number of devices requires more reliable energy solutions. For instance, PhyNetLab [7, 4] is an IoT based futuristic warehouse. Such a warehouse would be equipped with up to some hundreds of thousands nodes in a real application. When these entities are only equipped with battery, number of communication has to be strictly managed. Moreover, a very high success rate communication protocol is needed to avoid fast battery depletion. On the other hand, regardless of efficiency and quality of the communication, all batteries has to be replaced after their limited life cycle. This will introduce a large maintenance effort and cost that may threaten the feasibility of the whole IoT based warehouse solution.

To conquer the energy supply challenge for IoT devices, a continuous supply has to recharge batteries and avoid constant reduction of energy level. Energy Harvesting (EH) components are perfect solutions for such applications. An EH system provides a limited amount of energy per time, but in a continuous manner. Therefore, batteries would act more as an energy buffer that balances energy difference between supply and demand. In a well designed device there should be such a balance between the normal operation and the power supply. Therefore, the extra buffered energy would be fed to the system during

high demand events such as communication. Fortunately, most of these power demanding operations are short term. Therefore, the life cycle of CPS expands exceedingly by a proper balancing between communication intervals and harvested energy. In theory, such a system will have an infinite life cycle. Yet, the physical limitation of components such as energy storage or harvester itself will limit this time. However, in any case it would live much longer than an entity only powered by a battery.

There are multiple harvesting techniques available which can be used based on the field of application. However, PhotoVoltaic (PV) is the most widespread form of EH [8] and can be considered as the most mature solution among them. Therefore, PV is considered as the harvesting type hereafter.

Introduction of each EH to a CPS has its own requirements. First, it has to be considered that the collected power from a harvester is dependent on its operational condition. This is mostly a nonlinear dependency, leading to a dynamic performance. This nonlinearity for a PV cell can be simply seen in Figure 1.

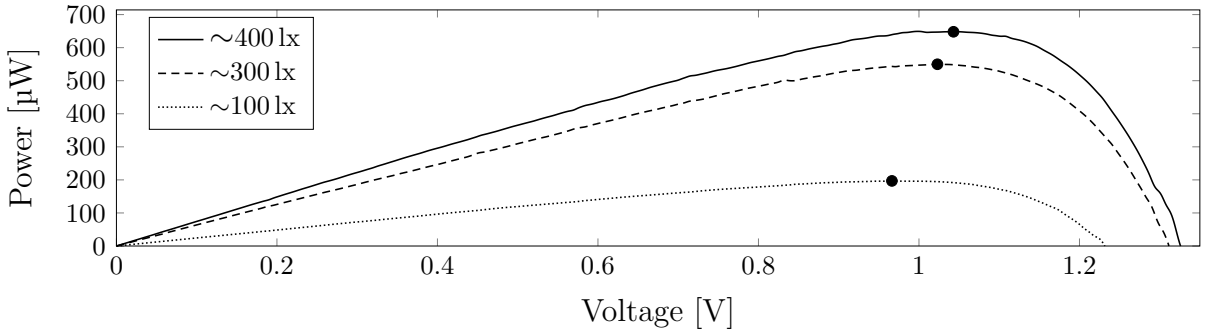


Figure 1: Harvested power from a Sanyo AM-1454 photovoltaic harvester under three different indoor lighting conditions

As marked in Figure 1, there is a single point with the maximum generated power for each operational condition. This point is commonly known as the Maximum Power Point (MPP).

For an ultra low-power IoT system, every bit of harvested energy is essential. Therefore, a harvesting system has to operate near the MPP. This task, commonly known as Maximum Power Point Tracking (MPPT) is a traditional challenge in the field of PV harvesting.

There are multiple techniques available aiming for MPPT [9]. The number of these techniques is so large that even some surveys are necessary to sort the publications for the categorization and classification of them. For instance, although [10] collected 30 techniques for MPPT, it had been extended in [11] to 62 methods.

In addition to the dynamic behaviour of the harvester, the storage voltage of an IoT entity changes continuously during its operation as well. This changes are dependent to the power delivered from the EH at one side and the current intake from the rest of the system on the other side. If harvester and storage be connected directly to each other, these voltage changes directly affect the harvester's performance. This performance reduction is mainly a consequence of the voltage mismatch between storage voltage and the MPP

voltage. To conquer this issue, a voltage matching system in between is necessary.

A voltage converter is able to keep the harvester's voltage at optimum while delivering power to the storage at its voltage. Considering all these requirements, the overall chain of energy supply would be as shown in Figure. 2.

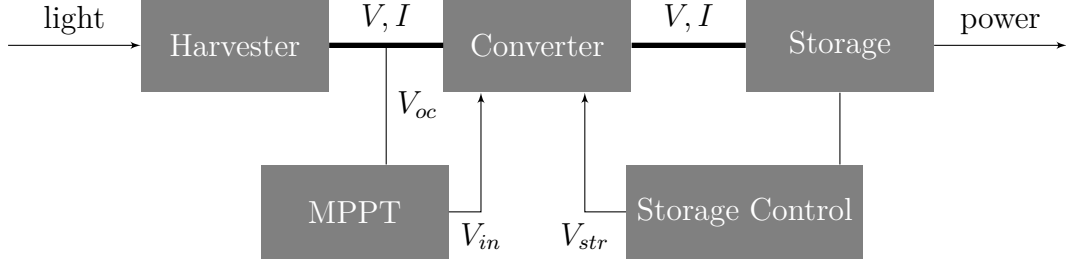


Figure 2: Complete power supply chain for an EH powered CPS

In this figure, connections between harvester, converter and storage have no direction. Although power is transferred from harvester in the direction to the storage, these physical parameters are bidirectional. For instance, the operational voltage of the harvester is affected by the converter through the MPPT process, though the power direction is from the harvester to the converter.

This overall structure has some more functionalities than only voltage conversion. In addition to conversion and MPPT, it also controls the storage. Therefore, it is more proper to call such a system a charger than only a converter.

Although the PV generated power is in the DC form, there are EH devices which provide an alternating current. In those cases, energy converter has to convert the harvested energy to a DC signal first and subsequently match its voltage level to the DC voltage of the storage.

MPPT algorithm has to be integrated in the converter system while it controls the EH's voltage. Accurate MPPT techniques require large computing resources and energy. In the outdoor application of the PV harvesting commonly known as solar energy, this algorithms are acceptable; because MPPT energy demand is smaller than the energy loss by operating at non-optimal voltage. However, these techniques are not feasible for most of the IoT applications. These devices operate mostly in indoor environments with ultra low harvesting potentials. Therefore, the energy demand for MPPT itself has to be very small compared to its marginal harvesting improvement.

This stingy intuition to the energy overhead has to be kept for the power conversion as well. Many different converters' designs are available promising different efficiencies with diverse field of application. Among this vast number of designs, switching based techniques are preferred mainly because of their better efficiency.

Available switching based converters have diverse efficiencies for each working range according to their switching algorithms. However, converters with Pulse Frequency Modulation (PFM) switching strategies provide a better performance for the ultra low-power range. [12]

Some IoT designers develop their ad-hoc conversion solution specifically designed for

their entity. However, having MPPT, battery control, converter and switching logic would require a series of components. These devices will increase the initial cost and the overall energy loss overhead of this middle-ware between the EH and the storage. Nevertheless, these issues can be conquered by integrating all these elements and logics into one single chip. Currently, there are three Texas Instruments (TI) chips from the BQ255XX series and ST (SPV1050) chip available off-the-shelf, specially designed for low energy environments. Among them, TI's BQ25505 and BQ25570 chips promise a better performance out of the box and are dominant in the market.

Although multiple designers have used these chips in their IoT devices, no analytical analysis on them is available. Some basic information about these devices are available through their datasheets [13, 14]. However, for a reliable design and fast analysis of the overall energy performance of an IoT device, these chips have to be modelled.

2 Modelling principles

Available modelling techniques can be categorised according to multiple aspects. One of the most common categorisation is based on the level of knowledge from the internal operation of the modelled system. This perspective divides modelling techniques into three groups as followings:

2.1 White-Box Modelling

When the whole internal configuration and relations of a system is being expressed by the model, it is called *White-Box Modelling*. This method is commonly known for modelling multiple physical principles.

Using Newtonian mechanics for formulation of force, acceleration and speed of an object is a common form of this modelling view.

2.2 Black-Box Modelling

When the exact detailed internal vision from a system is not available, a data based perspective has to be used. The most common modelling technique relying on the data from a system is the *Black-Box Modelling*. In the black-box modelling, internal structure of a system is completely ignored and model is only based on the relations between its inputs and outputs (IO).

This type of modelling is commonly used by control engineers for designing observers and controllers for complex industrial applications.

2.3 Grey-Box Modelling

Although black-box modelling perspective is useful for some applications, its extreme level of abstraction provides limited information for some use-cases. Therefore, there is a third category of modelling techniques called *Grey-Box Modelling* which fits in between the two aforementioned methods. In this category some internal knowledge about the interiors of the system is available. This is commonly a parametric model declaring some relations¹ of different internal parameters. However, these parameters are unknown and have to be identified using implementation of the parametric model using IO data. Moreover, outcoming model has to be evaluated for different working areas of the system to avoid unseen internal substructures and hidden behaviours.

2.4 Modelling techniques for converters

Generally, no chip manufacturer releases a detailed version of its product interior, at least as long as it is active. The TI chips BQ25505/70 are also not excepted from this general rule. Therefore, a white-box modelling is not possible and data-based techniques has to be used. Since datasheets provide an abstract understanding of these devices, a grey-box approach would be preferred.

3 Motivation

As mentioned, data based modelling methods rely on the collected data from the system. Therefore, an accurate reliable set of data for modelling in addition to another independent dataset for evaluation of the model are necessary. Generally, getting enough data for an accurate model is a challenging task. It has to represent the whole system and interaction of its internal parameters using different combination of IO signals.

This paper provides a general roadmap for collecting this data for modelling DC-DC converters for implementation in ultra low harvesting applications. Although TI BQ25505/70 chips are used during the procedure, this structure can be used with slight modifications for other chips or even non integrated converter devices as well.

The rest of this paper is structured in a way that an abstract explanation of TI ultra low-power chargers is explained first. Afterwards, configuration of the measurement platform including measurement device, chargers board and their connection is presented. Specification of measurements is given later on. Next, two separate experiments are defined for modelling and evaluation of the model. Subsequently, analysis techniques for the collected data and its post processing is provided. Finally, data storage is explained shortly.

¹These are not all possible internal relations. Each model has its own purpose and should be valid for its desired application. Therefore, ignoring some internal relations of the system is acceptable as long as the overall goal of modelling is intact.

4 Device specifications

Any data-based model is only valid within the range of the data it is made from. On the other hand, a reliable model has to include information for all its possible working points. Therefore, measurements has to provide information for the whole operational range. Consequently, information about the operational range of a device is required before experiments designing.

For the current case explained here, some essential data about the device can be simply collected from the manufacturer's datasheet.

4.1 Internal state machine

Based on the information from datasheets, operation of these chargers can be presented with a state machine as shown in Figure 3.

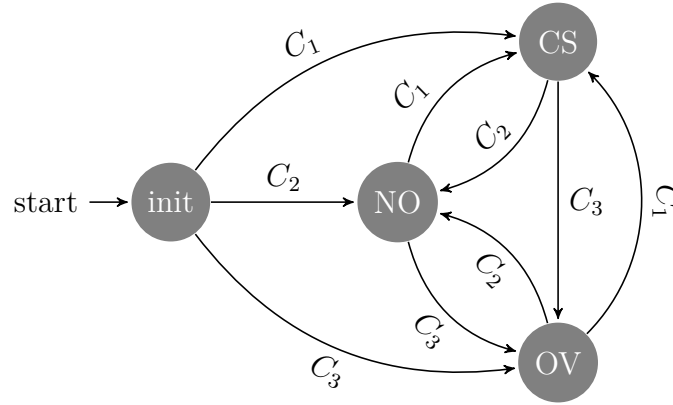


Figure 3: A simplified state machine representing charger's operational states

Three operational states are available in these chargers as:

CS: Cold Start is when there is not enough voltage to run the internal MPPT circuit. Therefore, input voltage is cut to 330 mV.

NO: Normal Operation is when the MPPT circuit is operating while the required storage voltage is available and the system is running normally.

OV: Over Voltage protection is when the maximum user defined storage voltage is reached and the charger disables any further feed to the storage.

To change states, three transition conditions are foreseen, all relying on the storage voltage (V_{str}) as:

C_1 : $V_{str} < 1.8 \text{ V}$

C_2 : $1.8 \text{ V} < V_{str} < V_{ov}$

C_3 : $V_{ov} < V_{str}$

where the maximum allowed voltage of the storage (V_{ov}) can be defined by the user according to the desired hardware specifications.

A converter relies on its MPPT system from its input side and battery control on the output side. Therefore, these two aspects are explained with more details.

4.2 MPPT

These devices such as many ultra low-power harvesters rely on fractional methods among different MPPT techniques. Fractional methods are built on the fact that the MPP is usually a fraction of some parameters of the harvester. Consequently, this parameter has to be sampled continuously. While continuous measurement will increase the energy overhead, sample and hold principle [8] is used for ultra low-power applications.

In addition to low operational energy demand, this technique is a direct technique and requires no prior knowledge from the harvester. This makes its implementation favourable without worrying about the exact parameter values, operational condition and harvester's production tolerances.

Two well known fractional methods used for the PV harvesting are Fractional Open Circuit Voltage (FOCV) and Fractional Short Circuit Current (FSCC). The FOCV can be simply formulated as:

$$k_v = \frac{V_{mpp}}{V_{oc}} < 1 \quad (1)$$

Although this fraction had been reported to be between 75 % to 80 % of the open circuit voltage (V_{oc}) for PV harvesters [15], finding the exact fraction value is a challenging issues [9].

The same principle is reported that the current at the MPP is a constant fraction of the short circuit current (I_{sc}) as:

$$k_i = \frac{I_{mpp}}{I_{sc}} < 1 \quad (2)$$

and the suggested value for the current fraction constant (k_i) in PV application is mostly about 85 % [9].

In most cases, current measurement is done by measuring voltage at both sides of a shunt resistor. Then the current is calculated based on the voltage difference and the prior knowledge about the resistant value. Therefore, FOCV is preferred for the ultra low-power applications. FOCV would be faster, requires less hardware and demands less energy compared to the FSCC.

TI also uses a sample and hold FOCV MPPT algorithm. The exact k_v fraction can be set using two external resistors. In addition to the 75 % to 80 % for PV harvesters, TI datasheets [16, 17] suggest a 50 % fractional value for thermoelectric converters.

The sample and hold process of detecting open circuit voltage repeats every 16s and each MPPT measurement of V_{oc} takes 256 ms. However, as shown in the state machine of the

charger in Figure 3 this process happens only when there is enough voltage provided from the storage side in the NO state.

4.3 Battery Control

Both TI chargers are designed to support different storage mediums. It can be a rechargeable battery, super capacitor or even a simple conventional capacitor. Storage acts as a buffer to handle demand peaks that the harvester cannot directly feed. Therefore, this energy storage has to be protected on both extreme cases of over and under voltages. Although under-voltage limit is internally programmed in these chips, over voltage level can be programmed externally by user. Moreover, a flag signal generated by charger provides the possibility to inform the IoT device for the battery good condition [13, 14].

In addition to the voltage provided from the storage, the BQ25570 is able to provide a secondary regulated supply via its buck converter. This supply can be programmed externally and is able to provide an output with high efficiency. Its output may be as low as 10 μ A to high currents up to 110 mA [14].

An abstract collection of other key specifications for TI BQ25505/70 chips is presented in Table 1.

Table 1: Key operational parameters of TI BQ25505/70 from [13, 14]

specification	min	nom	max	unit
Input DC voltage	0.1	-	5.1	V
Input capacitance	4.7	-	-	μ F
Storage capacitance	4.7	-	-	μ F
Storage/battery(equivalent) pin capacitance	100	-	-	μ F
Input inductance	22	-	-	μ H
Total MPPT setting resistance	18	20	22	M Ω
V_{oc} for 80 % MPPT	$V_{str} - 0.015$	-	-	V
V_{oc} for 50 % MPPT	-	-	15	mV
Charger's cycle-by-cycle current limit ^a	-	230	285	mA
Input power for normal charging	0.005	-	510	mW
Maximum charger switching frequency	-	1.0	-	MHz
Storage voltage to switch from CS to NO	1.6	1.73	1.9	V
Minimum CS input power	-	15	-	μ W

a) at storage voltage 4.2 V, input voltage between 0.5 V to 5 V

5 Measurement configuration

In normal operation, charger would be connected to a harvester from the input side and a storage device at its output. Collected data for modelling has to provide information for all possible working points of the charger according to the harvester and the storage.

To collect this data, both these elements should envelop their operational range during the data collection process. In addition, this has to be carried out in a controlled way.

It is possible to force the storage voltage into a special value by use of an extra demand current. However, this would require a complex closed loop control system to keep this value constant during a measurement. Moreover, it adds some fast dynamics to the system and may compromise collected data.

In addition, forcing a PV harvester to work under different conditions and keeping it stable is extremely hard if not impossible. This requires a complex modifiable light measurement unit such as presented in [3, 18]. Even such measurement platforms have limited working range which may lack some operational points of the harvester or converter. It would be better to mimic the key aspects of a harvester to analyse the converter's behaviour without any effect from the rest of system.

Hence, some extra devices has to reproduce the behaviour of the harvester and the storage but in a completely controlled manner.

A PV energy harvester behaves mostly as a current source with a nonlinear relation according to its voltage. This behaviour is shown in Figure 4 for a Solems PV cell measured under some indoor lighting conditions.

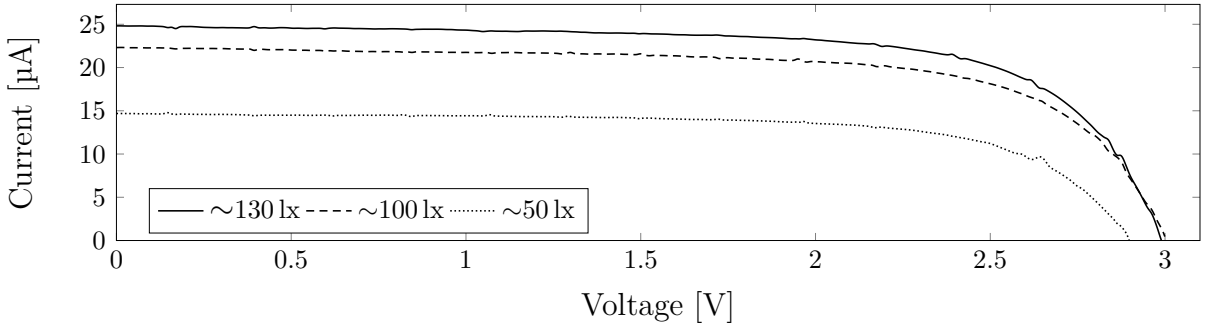


Figure 4: Voltage-current relation of a Solems cellule solaire Ref.05/048/032COA PV harvester measured under three indoor lighting conditions

There are some specific devices able to reproduce such exact curves. Even though, reproduction of such curves is not necessary for the modelling. A converter only requires the open circuit voltage from the harvester to calculate the MPP. Accordingly, in addition to the current source value, the only critical parameter is the open circuit voltage.

A charger's model has to be independent from harvester's behaviour, while it has to be valid for all different kinds of harvesters.

The current source will represent the PV generated current and the open circuit voltage V_{oc} can be reproduced by the compliance of the source. By setting different current values and compliance voltages, it is possible to reproduce key parameters of many PV cells and analyse the converter's conduct for them.

On the storage side, the same principle can be implemented. The only critical parameter required from a storage is its operational voltage value. It can be simply reproduced

by a voltage source. Also, the maximum allowed current (before it burns out) can be implemented as a current compliance.

Simultaneous to mimicking input and output by sources and compliances, the voltage and current signals has to be measured as well. Therefore, a device able to provide a current source and a voltage source while measuring the voltage and current at both these channels is required.

5.1 Hardware

Before starting with the data collection, required hardware has to be prepared and connected with each other. A short description of these devices is explained here.

5.1.1 Source Measurement Unit

As mentioned, one current source at input side representing the harvester and a voltage source representing the storage are required. Voltage and current has to be measured simultaneously on both sides as well. Based on these specifications, a Source Measurement Unit (SMU) with two channels is required. A SMU has the benefit of accurate measurement while acting as a source.

As shown in Figure 4, some PV harvesters provide very small current as low as few micro ampere in the indoor applications. Therefore, current source of the SMU has to be able providing such low values. Moreover, its measurement has to be as accurate as one tens of the lowest current value to assure acceptable measurement of all signals. Considering maximum internal switching frequency of 1 MHz, SMU has to have measuring frequency capability of at least 3 MHz to fulfil Nyquist sampling theorem. Based on all these specifications, two SMUs from *Keysight* with model numbers *B2902A* and *B2962A* are selected.

These devices are from the same family of the same producer equipped with two channels. They are able to source current from 10 fA to 10.5 A and voltages in the range between 100 nV to 210 V with the maximum 31.8 W power. Measurement precision of both devices is 10 fA and 100 nV [19, 20]. Although both devices allow user defined source signal generation, B2962A has more predefined source signal forms out of the box. Furthermore, they both support Standard Commands for Programmable Instruments (SCPI) commands for communicating with a computer. This makes a systematic data collection controlled by a computer program possible. In addition, both devices are calibrated by authorized personal for an accurate measurement.

5.1.2 Charger board

Ultra low-power charger chips provide all required functionalities integrated in one device. However, some extra components has to be added for normal operation of them. Resistors for MPPT fraction definition, capacitors for noise filtering are some examples of these components. Although it is simply possible to build up a running board for

each chip, use of a certified board would be preferred. While the collected data would be used as a modelling reference, evaluation boards *BQ25505-EVM* and *BQ25570-EVM* manufactured by TI are used for measurements. These boards provide a unified certified running system which would be the same for all users. This avoids any problem due to failure in the self production of the boards.

Schematic representation of both evaluation board is presented in appendices. Further information about these boards can be accessed through TI datasheets in [16, 17].

5.2 Connections

For the measurements, SMU channels are connected to the jumper connections of the evaluation boards as:

- SMU Channel 1 positive, to “VIN” from J1
- SMU Channel 1 negative, to “GND” from J2 or J3
- SMU Channel 2 positive, to “VSTOR” from J4
- SMU Channel 2 negative, to “GND” from J6

The overall hardware configuration would be a simple system as shown in Figure 5.

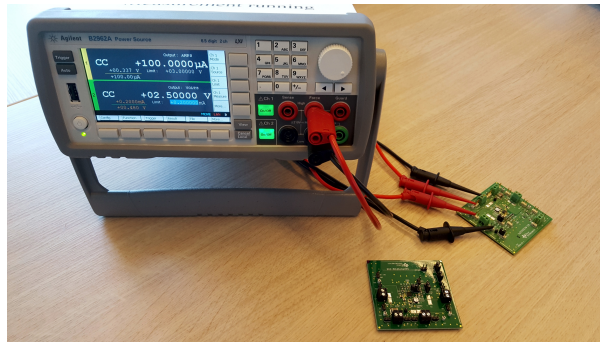


Figure 5: The overall required hardware, including SMU and two evaluation boards

For the automatic data collection, SMU is connected to a PC through a USB or network connection. On the user PC, a MATLAB® software is installed. It is able to communicate with the SMU in both directions transferring data and SCPI commands. A MATLAB .m program on the PC sends settings to the SMU, waits for the measurement to be finished and reads the collected data. It stores data and prepares the system for the next measurement. This process makes a systematic data collection possible as it is also for a mass data collection such as what is required for this application.

5.3 Measurement specifications

To collect data, different aspects of a system have to be considered. Data collection experiments and their description would be defined based on these specification explained hereafter.

5.3.1 Signal types

Input and output voltages, currents and powers are the key parameters for modelling. Since power can be reproduced using voltage and current, only these two parameters are measured. Consequently, four signals including two voltages and two currents are considered. All these signals has to be measured during an experiment.

In addition to the type and direction of signals, dependency of each signal has to be defined. Independent signals are forced by the user, while independent values are only measured. In addition, independent signals define the specification of sources.

Charger's input current is defined by the current source from channel 1 representing the generated current from a PV harvesting. The input voltage of the converter is not a fixed value. However, there is a maximum value for that which is the open circuit voltage of the harvester. This value is implemented as the voltage compliance for the current source.

A voltage source from SMU's channel 2 is connected at the output side of the converter. This voltage is the representation of the storage voltage. Output current is a dependent value which relies on other parameters and internal behaviour of the charger. No specific compliance for the current at the output channel can be considered except for the maximum allowed current of the storage.

5.3.2 Signal range and accuracy

Level of the collected data granularity determines the level of details in the model. Moreover, polluted data as a consequence of stretching a system beyond its functionality limits can compromise the resulted model [21]. Hence, range of signals and the accuracy of the collected data has to be analysed carefully.

Using abstract information provided in Table 1, the input voltage range of measurements may vary between 0.1 V to 5.1 V. Moreover, the maximum input charging power of 510 mW limits the current range to 100 mA with the maximum input voltage of 5.1 V.

Output voltage of the converter is connected to the storage. Based on the device information, output (storage) voltages up to 5.5 V are allowed. However, the default over voltage limit for the evaluation board is 4.2 V which is used here as well.

The minimum storage voltage may theoretically go as low as zero. However, when the storage voltage is lower than 1.6 V, device goes into the cold start state. In the cold start mode, MPPT does not operate and a fixed input voltage of 330 mV is implemented. Consequently, the storage's voltage has no further importance. Therefore, the minimum storage voltage of 1.5 V would be logical to analyse all possible conditions. Also, storage

voltages between 1.6 V to 1.5 V provide information from the cold start condition.

5.3.3 Measurement frequency

There is always a question of how much data is needed for the modelling purpose. Although collecting all data is always an easy answer, it is mostly impossible or extremely hard. To have all relationships at all levels in a system, enough data has to be collected. After all, enough data is when it contains all relationships of interest in the model.

In addition to the data collection points, frequency of sampling is a critical aspect of collected data size. A trade off has to be done to sample with the optimum frequency in a way that the required amount of data be collected and not more.

Most converters include switching electronics leading to some fast dynamics. When a time based model with all these fast dynamics is desired, measurement has to be faster than these dynamics to fulfil the Nyquist theorem. The internal dynamics of the switches in the TI converters can be as high as 1 MHz leading to sampling frequency higher than 2 MHz. However, in most IoT applications the stable behaviour or Periodic Steady State (PSS) model is preferred. Modelling PSS signals leads to a static model based on the operational condition and consequently is not time dependent.

Although measurement of PSS signals do not require fast sampling, single measurement of signals at a working point is also not enough. Presence of noise in measurement in addition to other dynamics in converters forces frequent sampling. The other interesting dynamic in the behaviour of a charger chips is the measurement of V_{oc} which lasts 256 ms. This information is required for understanding operational behaviour of the MPPT system. Therefore, sampling frequency has to be fast enough to provide enough redundant data from MPPT measurement periods as well.

Considering a sampling period of 50 ms, will provide up to 5 samples during MPPT measurement period. Hence, it is used as the sample time for the measurements representing a 20 MHz sampling frequency.

6 Data collection

Scope of each data collection has to be defined before starting with the collection itself. Within the context of modelling, two type of experiments are required. One set of data has to provide information about the PSS behaviour of the chargers, while another set would be used subsequently for the validation of the models.

These two sets have to be independent from each other to avoid any model compromise by over learning. Therefore, two independent experiments are designed for this application.

6.1 Modelling experiment

This experiment has to provide data from PSS signals at each operational point in addition to the MPPT values. A complete procedure of measuring all possible signals at

an operational point take as long as one complete period of MPPT which lasts 16s. However, noise during MPPT sampling may cause unreliable data. Collecting data for three MPPT periods will be a trade off to have enough reliable data at each working point. Consequently, a modelling experiment will be setting parameters for one operational point and measure all PSS signals for 1 min (about three MPPT periods) with a 50 ms sampling frequency.

Each charger has some initial internal behaviour. The exact reason for this first conduct cannot be explained without internal knowledge from the device. Yet, based on their dynamics, perhaps it is for charging some internal capacitors.

Collected data during this period is not valid while it is only an internal initialization dynamic and will not happen during normal operation. Consequently, this time is only a waiting time before each measurement.

In case any operational point be measured as a standalone experiment, this initialization time overhead will extend the required time for the whole measurement set. If a series of experiments run subsequently after each other, this extra time is not necessary for each single initialization. While the internal capacitors do not lose charge to be pumped up again after a new start.

In this concept, system starts in one combination of setting parameters and waits for the initialization time. Afterwards, measurement and data storage starts. Signals are kept constant for the desired period of 1 min. When this time is passed, one independent parameter changes instantly to a new value in a stepwise manner without disconnecting other sources from the converter or interrupting data collection. This stepwise change of parameter, sweeps the whole possible range of working points. At the end of the sweep, measurement is stopped and the collected data get stored.

The size of step changes within the sweep defines the accuracy of the model in the modelling phase. Smaller step sizes lead to more accurate models, though it increases the data collection time. A trade off has to be done between the time and accuracy of the model based on the step size.

To keep the data from this modelling data collection scenario comprehensible, only one of three possible independent parameters changes. Therefore, this experiment has to be repeated for all combination of other two parameters. This process is a time consuming scenario while actually three dimensions of parameters are being swept to collect all data for the whole possible working space.

To select the most proper parameter for sweeping, it is better to analyse the normal operation of an IoT entity. In a real scenario, nodes have a constant environmental situation while the stored energy in the storage and its voltage continuously changes. Therefore, the storage voltage (charger's output voltage) is considered as the changing parameter here while the other two factors are kept constant. Using this concept, the overall algorithm for this process is explained in Algorithm 1.

This algorithm is written in a very visual syntax. For each measurement device the proper SCPI commands for each task has to be written and transferred to the device in the right semantic.

Algorithm 1 Process of collecting the modelling data

```
1:  $T_s = 50$  ms; {Measurement sample time}
2:  $I_{in} = \text{xxx}$ ; {Supplied constant current}
3:  $V_{oc} = \text{xxx}$ ; {Open circuit voltage, compliance}
4:  $V_{s,Max} = 4.2$  V; {Maximum voltage on the storage side}
5:  $V_{s,Min} = 1.2$  V; {Minimum voltage on the storage side}
6:  $Step_s = 100$  mV; {Voltage change of each step}
7:  $Step_d = 1$  min; {Duration of each step}
8:  $T_{init} = \text{xxx}$ ; {Initialization time, dependent on the input current}
9: Connect to SMU; {Define port no., device ID, data rate, buffer size, ...}
10: Setting CH1 Source; {Constant current source}
11: CH1 Transition trigger: 'none'; {Signal is constant}
12: Setting CH2 Source; {Sweeping voltage source}
13:  $N = [(V_{s,Max} - V_{s,Min})/100 \text{ mV}] + 1$ ;
14: CH2 Number of transition trigger =  $N$ ;
15: CH2 Transition trigger period =  $Step_d$ ;
16: {Sampling specification}
17: Number of sampling trigger =  $(N \times Step_d)/T_s$ ;
18: Sample time =  $T_s$ ;
19: turn on 'CH1', 'CH2';
20: wait for  $T_{init}$ ;
21: turn on all triggers; {Transition and acquisition}
22: for  $T < N \times Step_d$  do
23:   Measure;
24: end for
25: turn off 'CH1', 'CH2';
26: read 'all measured data';
27: Store 'data', 'metadata' in MATLAB;
28: Disconnect SMU;
```

Using this process, a dataset for each combination of input current and open circuit voltage would be measured. One example of these collected data from a BQ25505 is presented in Figure 6.

As can be seen in Figure 6, it provides all critical signals for the whole measurement routine. The storage voltage (output of the converter) starts from 4.2 V and sweeps down stepwise to 1.5 V in 100 mV steps. This produces 28 voltage steps in each measurement set, each representing one possible operational point. One minute data is collected assuring three MPPT periods for each step. Considering the initialization time, each single measurement takes about half an hour. It has to be noted that the trigger of the measurement is planned in a way that the initialization time is not measured and can not be seen in datasets and this figures as well.

It is also possible to see in Figure 6 that every 16 s the MPPT algorithm detaches input, to measure the open circuit voltage. This produces a jump in the input voltage equal to the compliance voltage of the current source aimed to reproduce the V_{oc} of the PV cell.

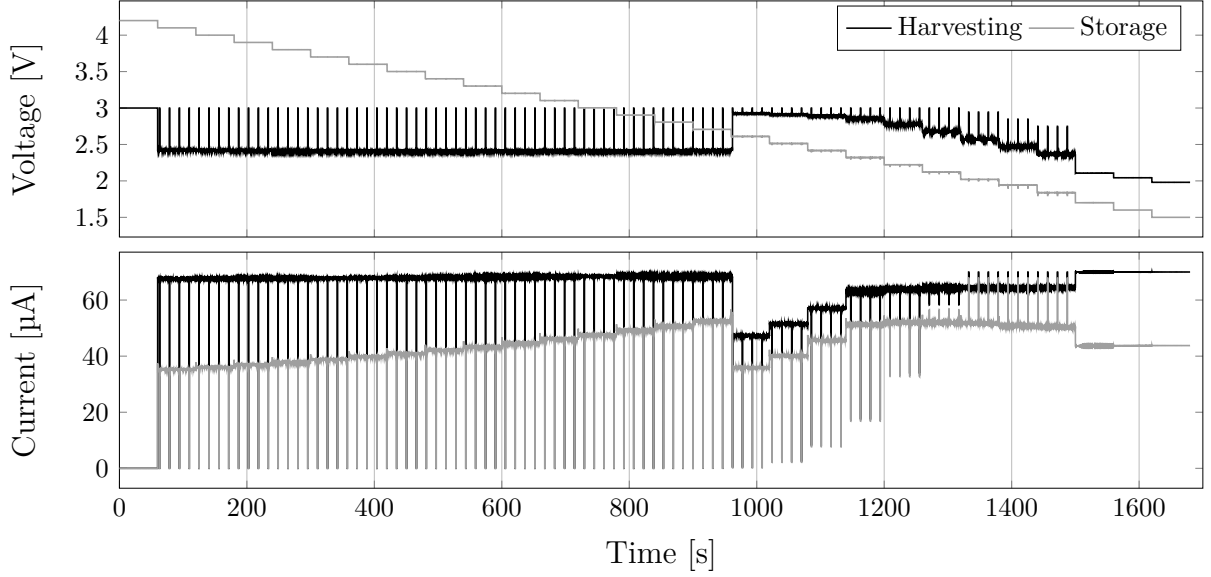


Figure 6: PSS signals measured from TI BQ25505 at constant input current of 70 mA and open circuit voltage of 3.5 V

The effect of this sudden change can be also seen in the input current signal is reduced to zero for this period.

This process is repeated for multiple input current source values from as small as 1 μA up to 100 mA. A graphical representation of all source current values is presented in Figure 7.

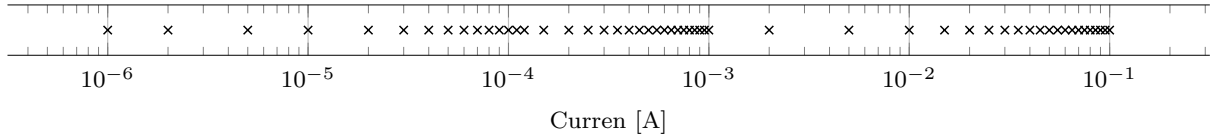


Figure 7: Graphical representation of all current values used for measuring datasets

Also, the open circuit voltage is changed in the range of 0.5 V to 5 V with 0.5 V steps. For each combination of these two parameters (source current and open circuit voltage) a dataset same as the example shown in Figure 6 is measured. It has to be considered that this procedure is done for both converters in the same manner. All in all, 540 datasets are measured for each device providing a sufficient set of data, spanning the whole possible working range of each charger.

6.2 Evaluation experiment

For any modelling procedure, some evaluation data is required in addition to the data used directly for the modelling. These datasets has to be independent from each other

to avoid unseen dynamics in modelling. Hence, a separate experiment has to be designed specially for the evaluation purpose.

As mentioned before, three possible parameters are available which define each operational point. In another word, the whole operational space of the converters can be considered as a three dimensional space. During the measurement experiments, these parameters were selected in a stepwise manner between two subsequent experiments. Therefore, data from last experiment are just some sample point from this overall space.

Data about multiple conditions in between those points from the modelling experiments are not known. Hence, it would be preferred to design evaluation experiment with a changing parameter in a continuous manner. Among those three parameters, sampling steps in both voltage parameters were defined in a very fine fashion. Providing much more information from these two parameters. Therefore, the input current is considered as the variable factor for the evaluation experiment data collection.

It is possible to change the current simply as an upward or downward ramp or an exponential. However, some systems show different dynamics according to the direction of changes in the signal. Therefore, a sinusoidal current signal is used. The benefit of a complete sinus cycle is that it goes through each possible point twice. Once in increasing manner and once reducing. This helps to reveal all dynamics of the converter, in case its dynamics are dependent on the sign of change.

The overall process of this data collection is similar to the one formerly mentioned in Algorithm 1. The difference is that in the evaluation experiments output side has a constant voltage value while the input side changes in one sinusoid cycle. This signal starts always at 50 mA and increases to the peak of 100 mA as the maximum allowed input current. After that, it is reduced to zero and again upward till 50 mA. The whole process takes 1000 s which is the maximum user defined non-constant input signal by the Keysight SMUs. The overall simplified algorithm for this process is presented in Algorithm 2.

The proper SCPI commands of each line of this visual algorithm has to be transferred through a common programming language into the SMU.

An example of the measured data using this algorithm for the TI BQ25570 is presented in Figure 8.

Since both voltages are kept constant during one experiment, multiple experiments are possible by modification of voltages. This experiment is repeated by changing the open circuit voltage in the range of 0.5 V to 5 V and storage voltage between 1.5 V to 4.2 V for both converters. Consequently, 280 sets of evaluation data is collected for each charger.

7 Data processing

Same as any other experimental data collection, these data are not free from noise and other measuring irregularities. Moreover, as can be seen in Figure 6 and Figure 8, the MPPT measurement procedure is also available in the data. These anomalies have to be removed for the normal operation condition of the chip though they are necessary

Algorithm 2 Process of collecting the evaluation data

```
1:  $T_s = 50$  ms; {Measurement sample time}
2:  $V_{oc} = \text{xxx}$ ; {Open circuit voltage}
3:  $V_{str} = \text{xxx}$ ; {Open circuit voltage}
4:  $Sin_B = 50$  mA; {Initial value of the sinusoidal current signal}
5:  $Sin_A = 50$  mA; {Amplitude of the sinusoidal current signal}
6:  $Sin_C = 1000$  s; {Duration of a full sin cycle}
7:  $T_{init} = 30$  s; {Initialization time}
8: Connect to SMU; {Define port No., device ID, data rate, buffer size, ...}
9: Setting CH1 Source; {Sinusoidal current source}
10: CH1 Number of transition trigger = 1; {Only one cycle of sin}
11: CH1 Transition trigger period =  $Sin_C$ ;
12: Setting CH2 Source; {Constant voltage source}
13: CH2 Transition trigger: 'none'; {Signal is constant}
14: {Sampling specification}
15: Number of sampling trigger =  $Sin_C/T_s$ ;
16: Sample time =  $T_s$ ;
17: turn on 'CH1', 'CH2';
18: wait for  $T_{init}$ ;
19: turn on all triggers; {Transition and acquisition}
20: for  $T < Sin_C$  do
21:   Measure;
22: end for
23: turn off 'CH1', 'CH2';
24: read 'all measured data';
25: Store 'data', 'metadata' in MATLAB;
26: Disconnect SMU;
```

for modelling some other specifications such as the MPPT behaviour itself. Therefore, filtering would be the first step before any further analysis.

Moreover, each modelling experiment dataset is a combination of multiple working points measured subsequently in one acquisition round. Hence, each modelling dataset has to be broken down into multiple separate single operational points.

7.1 Filtering

While operational condition of the charger is kept constant, measured PSS signals have to be constant as well. Any change in the signal which is not specifically defined during the experiment can be considered as a measurement noise. This noise can be simply seen in both examples shown in Figure 6, Figure 8.

A filter has to remove jitters in addition to the MPPT sampling period while keeping other changes in the voltage signal intact. Smoothing which is a commonly known filter is a moving average filter acting as a low pass filter. Although it removes small oscillations in the signal, it modifies the voltage changes as well which is not desired. This issue can

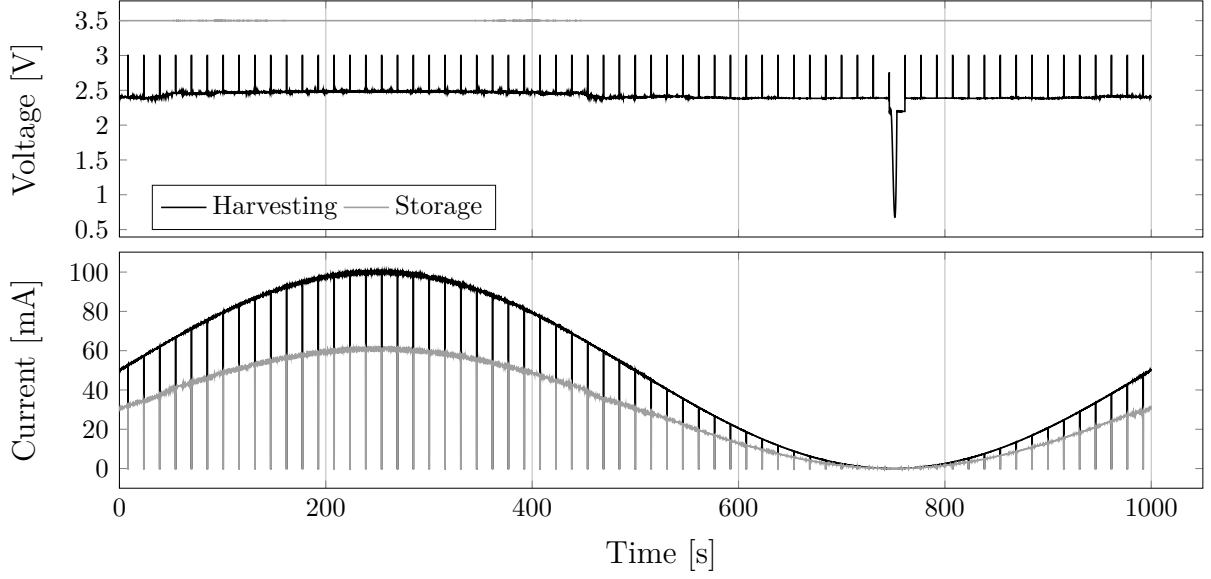


Figure 8: Example PSS signals measured from TI BQ25570 with a sinusoidal input current, 3 V open circuit voltage and a constant 3.5 V storage voltage

be seen in Figure 9.

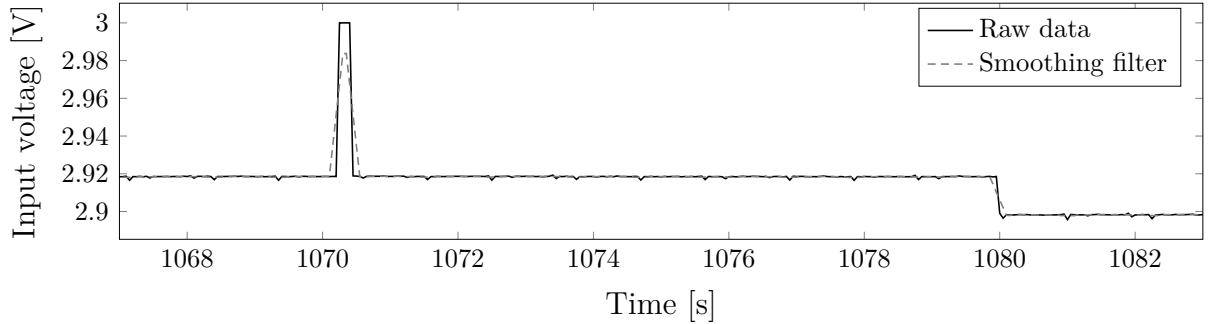


Figure 9: A smoothing filter changes voltage steps into a slope

However, a moving median filter can simply conquer this issue. Although it smooths out the signal to some extent, it keeps the steps unchanged and in the same time instant. While it uses the real measured values and not their average instead of them. However, the key to a proper moving median filter is selection of a proper moving window.

Removing the MPPT measurement pulse is a key desire of this filter. Based on the information from TI datasheet in [13, 14], MPPT sampling takes 250 ms. While measurement sample time is 50 ms. Consequently, there would be maximum 5 samples during MPPT measurement pulse. To remove these 5 samples, window size of the median filter has to be bigger than 5 at each side of this pulse. Therefore, a window size bigger than 12 would assure removal of the MPPT sampling pulse. To assure clean removal of the MPPT measurement pulses, a moving median filter with the window size 13 is used. This

is shown with $\mathcal{D}_{13}\{V_i\}$ where \mathcal{D} defines the use of median principle and 13 subscription shows its window size. Outcome of applying this filter on an example input voltage signal is presented in Figure 10.

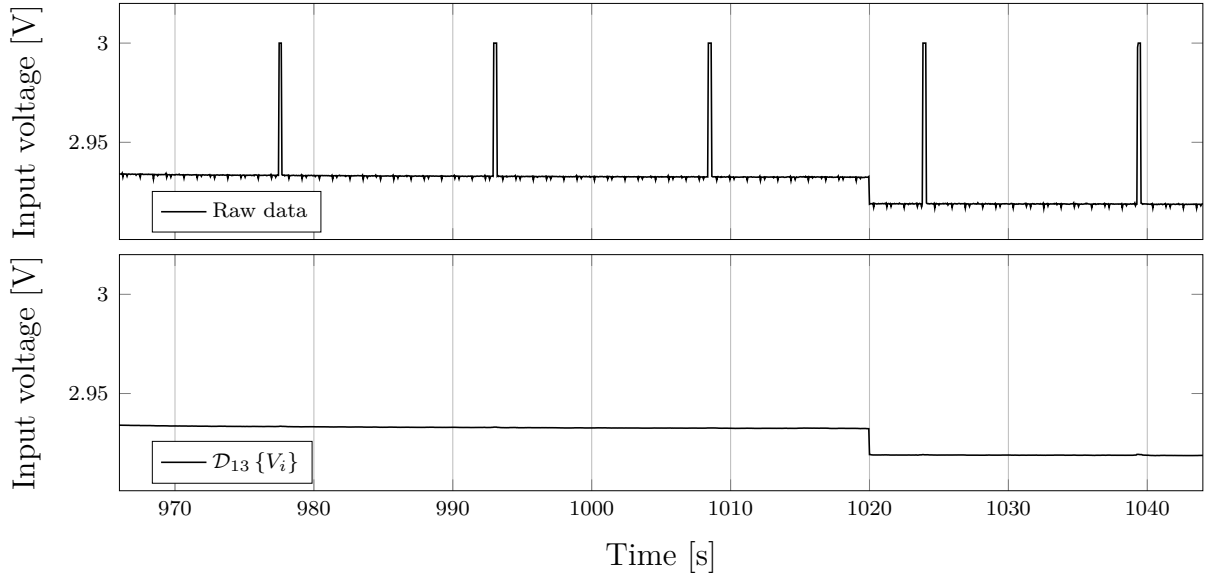


Figure 10: Filtered input voltage signal using a moving median filter with window size of 13 samples

7.2 Extraction

After filtering noise, jitters and MPPT measurement pulses from signals, modelling experiment has to be divided into its sub components. Each modelling dataset includes measurement of multiple operational points compressed into one experiment. Moreover, for each working point there are three periods of MPPT providing redundant data. Therefore, state of the system and operational status of each measured instant has to be detected. Any change of the operational state is a consequence of an event in one of the signals. Therefore, all events have to be detected.

7.2.1 Storage voltage change

During each modelling dataset, storage voltage changes in a stepwise manner. All steps have the same size of 100 mV. This signal is directly connected to the voltage source and has really small oscillations. Applying the same moving median filter used for input voltage filtration, will remove these sudden changes. These effect is shown in Figure 11.

To detect steps in the storage voltage, it is enough to check the difference of two subsequent signal instants in the filtered signal from the last step. Any difference bigger than 70 mV in this signal can be considered as a change in the storage voltage. This can be

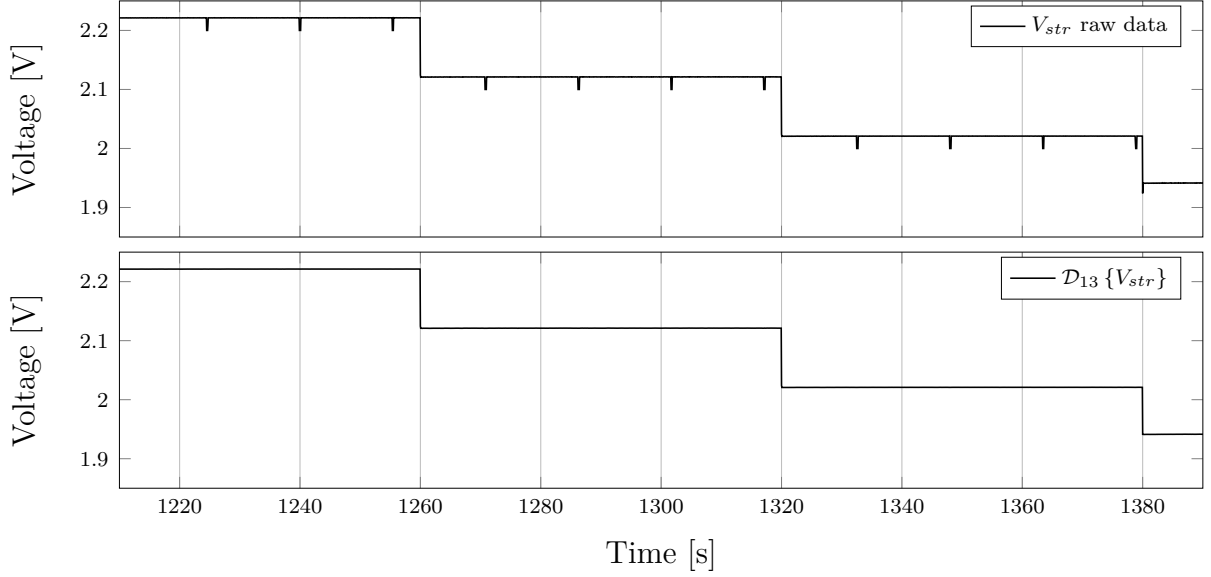


Figure 11: Filtered storage voltage signal using a moving median filter with window size of 13 samples

formulated as:

$$\mathbb{D}_{vs} = \{V_i \mid |\mathcal{D}_{13}\{V_{i-1}\} - \mathcal{D}_{13}\{V_i\}| > 70 \text{ mV}\} \quad (3)$$

where \mathbb{D}_{vs} is the set of sample instances with a change in the storage voltage $\mathcal{D}_{13}\{x\}$ is the moving median filter of x with the window size of 13 samples. Result of this detection for an example data is shown in Figure 12.

7.2.2 MPPT measurement pulse detection

During the filtration process, MPPT measurement pulses have been removed from the raw data. However, its starting and end time is the matter of interest in this step and has to be detected as events required for the system status detection.

As explained before, MPPT procedure is a time based series and repeats every 16s. Nevertheless, the starting point of this time series is dependent on the internal state of the chip and cannot be predicted. Consequently, the starting point of this series can happen at different point of time according to the experiment. Therefore, it is possible to consider the MPPT as a random behaviour which has to be detected and removed from the data. Based on these specifications, MPPT measurement pulses fit into the definition of outliers.

According to [22], outliers can be classified into three different categories as:

Point outliers: when an individual data outstands in respect to the rest of data.

Contextual outliers: when data is anomalous according to its specific context.

Collective outliers: when a collection of data is anomalous regarding the whole dataset.

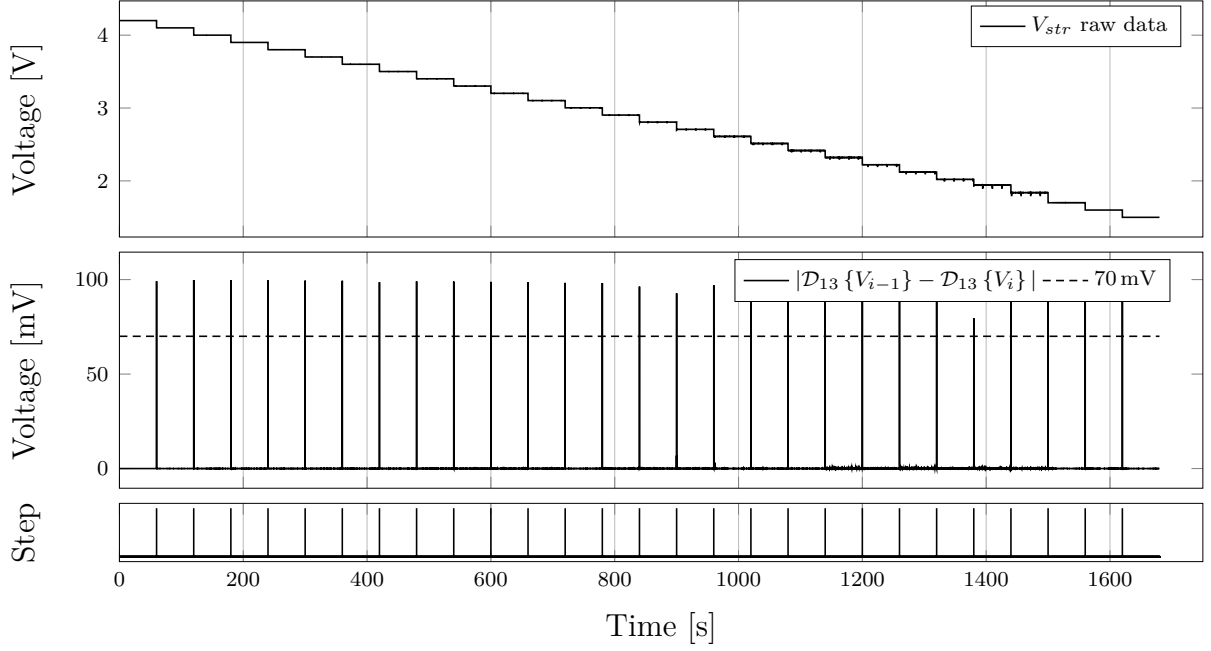


Figure 12: top: storage voltage, middle: difference of two subsequent filtered data samples, bottom: time instances with voltage difference values bigger than 70 mV

Although point outlier occurrence is possible in any data type, collective outliers are only in related instance data possible [22]. The MPPT sampling pulse is a set of related data which has an anomaly to the rest of the data for a single operational point. Therefore, it fits into the collective outlier definition.

Different outlier detection methods provide label for each data instance which can be a level of outlying from the rest or just a boolean marker pinning the exact outliers. While detection of MPPT measurement periods is desired here, a boolean marker is preferred.

Although conceptual definition of outlier explains their specification, a clear mathematical criteria for detection of outliers is required here. Multiple explanation and detection methods of outliers can be found in [23]. However, these methods compare each data instant to a specific bound. Among different values for this limits, a simple technique explained in [24] is the Median Absolute Deviations (MAD) defined as:

$$MAD = \text{median}(|x_i - \text{median}(x_i)|), \quad i = 1, 2, \dots, N \quad (4)$$

where N is the size of window used for calculating the median.

Using this definition, a data instance is an outlier when its value is more than three (or more) scaled MAD from the median. This type of outliers are shown using $\mathcal{O}_{13s}^d\{\bullet\}$, where d defines use of median and subscript shows the length of window for calculation of the limit bound.

It is also possible to use the same concept with the averaging of the values in a window and define outliers when the value is more than three standard deviations from the mean. This type of outliers are shown using $\mathcal{O}_{13s}^m\{\bullet\}$.

While a collective outlier is considered here, a window has to be defined which moves over the data through the time for calculation of the median and mean. Selection of this window size has to be analysed before implementation on the whole datasets. Using a window size of 13 samples same as filtering does not work properly. It can be seen in Figure 13 that such a small window size is very sensitive to noise.

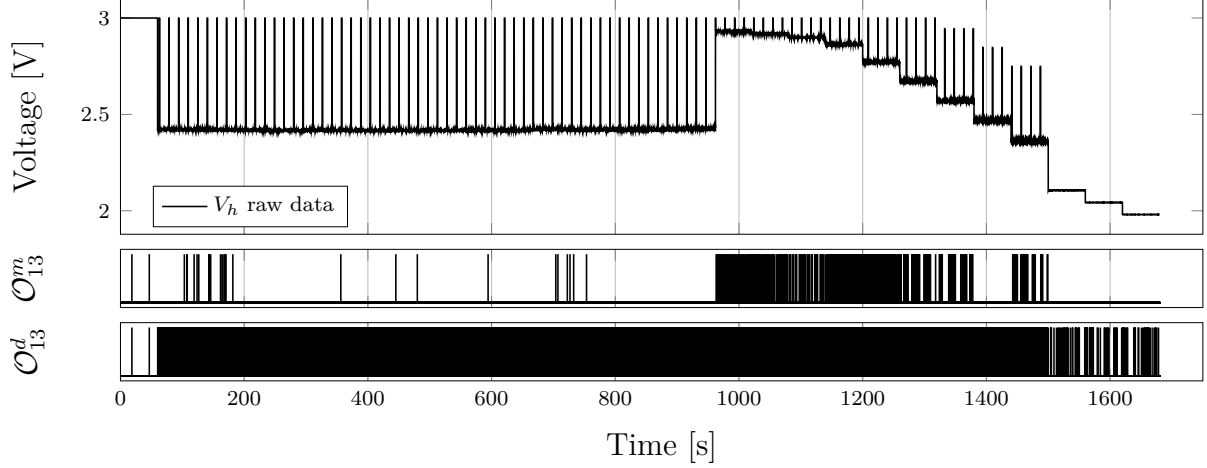


Figure 13: A direct implementation of outlier detection using moving mean and median with the window size of 13 samples

Although it is possible to change the detection criteria from three time to a higher value, this value should be fine-tuned for each single dataset. Moreover, detection using median is much more sensitive to small oscillations in these data compared to the mean value. To conquer these issues, a mean method with two window size of 16s, 30s are tested. Window size of 16s is large enough to include a whole period of MPPT. While the window size of 30s is large enough to include about two MPPT periods with only one MPPT sampling pulse inside the window. Results of this detection method using both window sizes are shown in Figure 14.

Although both of them detect about every MPPT measurement pulse, as can be seen in Figure 14, they still have problem for detecting the MPPT measurement pulse at about time 960s. This is mainly a consequence of the voltage change scale before and after the MPPT measurement pulse at this time instant and its scale compared to the open circuit voltage. Unfortunately, different trials on data using modification of window size shows no further improvement.

To solve this issue, data is normalized to remove the effect of its scale. Therefore, at first the difference between raw signal and filtered signal (using the moving median $\mathcal{D}_{13}\{V\}$ from last part) is calculated. Afterwards, the same outlier detection method using the moving median with a 30s window is applied. Result of this methods is shown in Figure 15.

As presented in Figure 15, an outlier detection using a moving mean on a 30s window of the absolute value of the difference signal will detect all MPPT sampling pulses.

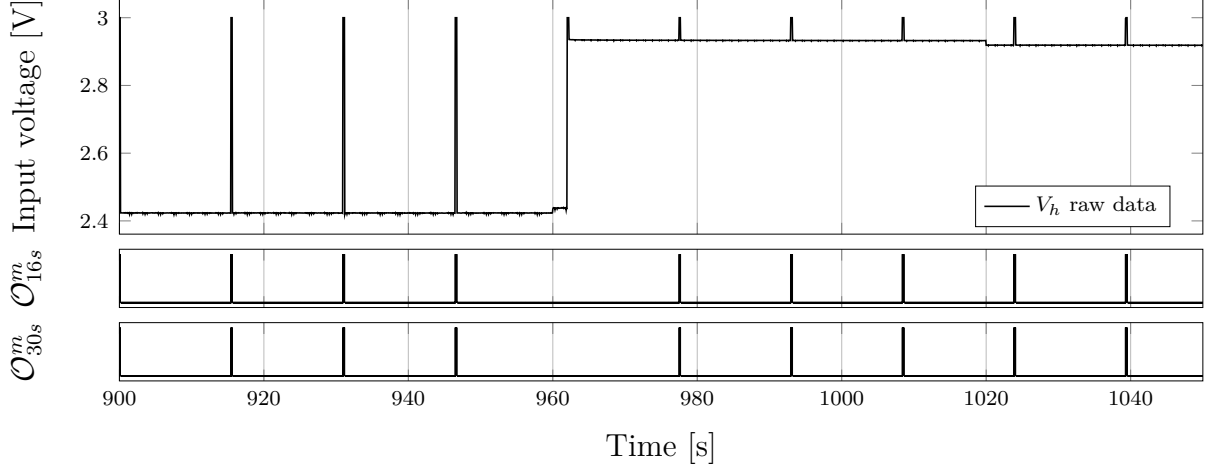


Figure 14: Implementation of moving mean outlier detection with two different window sizes

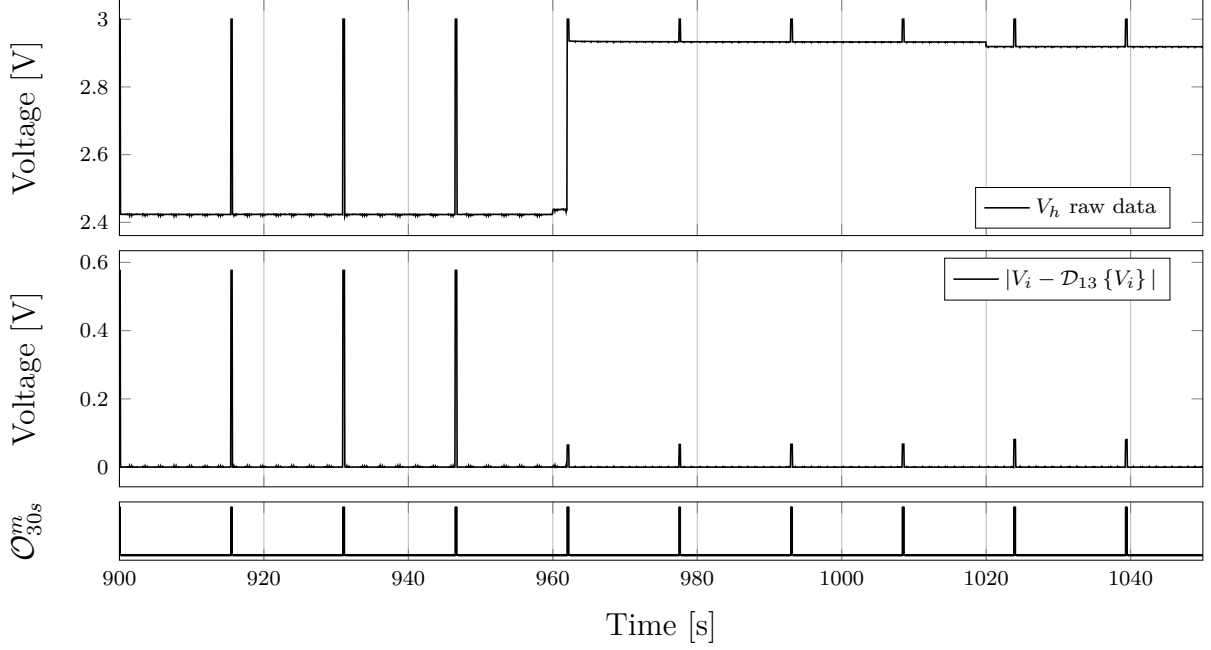


Figure 15: A proper implementation of outlier detection on the normalized difference input voltage signal

7.3 Labelling

After extracting all events in a dataset, data sections which have the same specifications have to be labelled and considered as a single sub-dataset. Each period of data has to be marked with two labels explaining charger's state and its operational condition.

7.3.1 System state

As presented in Figure 3, TI's BQ chargers have three operational states including *cold start* (CS), *normal operation* (NO) and *over-voltage protection* (OV). Switching between these states is only dependant on the voltage level of the storage. Therefore, this specification from the data can be directly extracted from the storage voltage.

By checking the storage level voltage for each set, charger's state label can be defined. A 4.2 V is used as the maximum allowed voltage and any higher storage voltage is in over-voltage protection. When storage voltage is between 4.2 V to 1.75 V, normal operation is running. Also, cold start label is defined when the storage voltage is smaller than 1.75 V.

7.3.2 Operation state

Operational states are another categorization of possible conditions

MPPT measurement: the period of sampling open circuit voltage.

Normal operation: when MPPT measurement is finished, the exact MPP condition is applied and the input condition is not changed.

voltage mismatch: duration of time that the input voltage is changed while the MPPT logic holds the last value. Converter is not working at optimal harvesting operation point during this time.

MPPT measurement and normal operation can only happen during the NO state of the charger state. However, voltage mismatch may happen during all three charger states.

Each period of data has to be defined using extracted events from the last part. By analysing events in a timely manner, each period between two subsequent events can be labelled accordingly. The overall process of period detection can be simplified as presented in Algorithm 3.

Graphical representation of all operational states for an example dataset is presented in Figure 16.

Each experiment dataset is broken down to its smallest pieces with all the signal values and operational condition labels.

8 Data storage

After defining each period's label, a simple averaging of the signal values in the period provides a reliable data representation of that specific part. This data is added as an entry in a list. Each entry row has all four averaged signals in addition to two labels defining the operational and charger's state labels. This procedure is applied on both 540 modelling datasets of each charger separately. By merging all collected data, a list with more than 100 000 entries is prepared for each device. Each list provides a collection of

Algorithm 3 Labelling system condition

```
1: LastEvent  $\leftarrow$  'voltage-mismatch' {no initial MPPT}
2:  $t = 0$ ;
3:  $\Delta t = 50$  ms;
4: while  $t < t_{max}$  do
5:    $t = t + \Delta t$ ; {next sample}
6:   if MPPTStart := true then
7:     Label  $\leftarrow$  'MPPT'
8:   else if MPPTEnd := true then
9:     Label  $\leftarrow$  'Normal Operation'
10:  else if VStorageChange := true then
11:    Label  $\leftarrow$  'voltage-mismatch'
12:  else
13:    Label  $\leftarrow$  LastLabel
14:  end if
15: end while
```

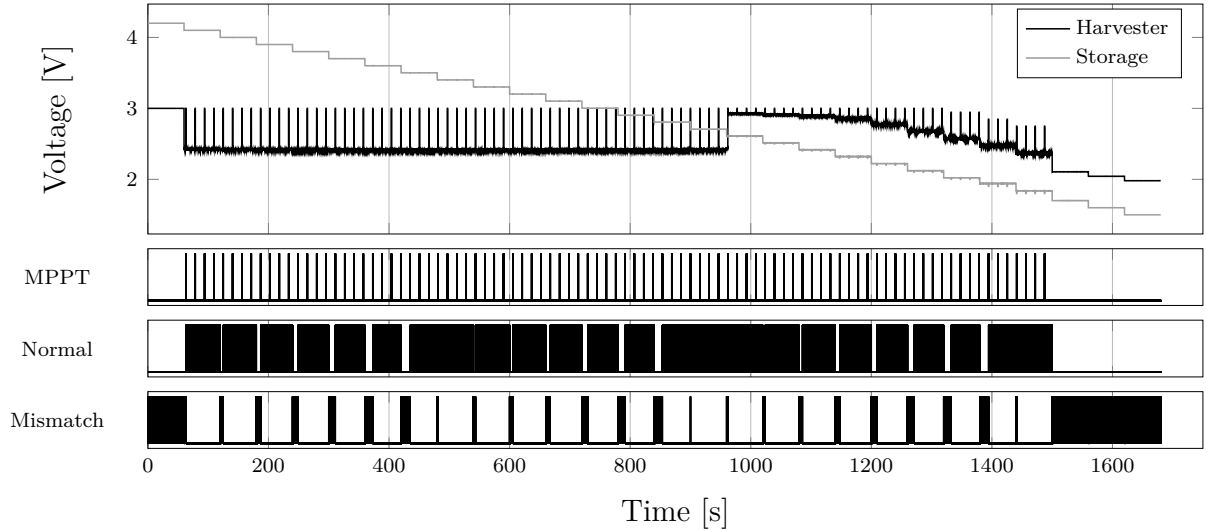


Figure 16: Graphical representation of all operational labels during one modelling measurement dataset

PSS signals in a wide operational range of the related device and can be directly used for the modelling purpose. At the end, each dataset including raw and filtered data, measurement meta-data in addition to all labels is stored separately.

9 Conclusion

Power conversion between energy harvesting and energy storage modules is a critical aspect for the future of IoT devices. It assures (near) optimal operation of the harvester and improves the overall energy harvesting and storage process.

For a proper design of the IoT energy supply, understanding this charging mechanism is necessary. Hence, a detailed analytical model of the charger would be the ideal solution. For the modelling purpose, all possible working points of a charger has to be analysed.

Although multiple ad-hoc solutions for power conversion are available, only few off-the-shelf chips are available with promising results for low-power harvesting. This work focuses on two most recent Texas Instruments ultra low-power chargers, namely BQ25505 and BQ25570.

To collect reliable data from these charger chips, an accurate source measurement unit represents harvester and storage behaviour in a totally controlled way. A SMU is able to measure signals as well while it is acting as a source simultaneously.

An automatic data collection process is designed measuring voltage and currents of each device at each operational point. During these experiments, the input voltage and current are kept constant and the storage voltage is changing as the independent parameter. For each device 540 sets of different operational points are measured. The data is filtered, labelled and prepared for modelling. At the end, a list of more than 100 000 operational data instances for each device is collected.

Another automatic data collection process is designed. This experiment uses a sinusoidal input current as the independent parameter spanning the complete range of possible currents. This provides evaluation data which is independent from the modelling data. For each device 280 sets of evaluation data is collected.

All in all, the overall collected data would be enough for black-box or grey-box modelling techniques to model these two ultra low-power chargers.

References

- [1] J. Venkatesh, B. Aksanli, C. S. Chan, A. S. Akyürek, and T. S. Rosing, “Scalable-Application Design for the IoT,” *IEEE Software*, vol. 34, no. 1, pp. 62–70, Jan. 2017.
- [2] M. Magno, V. Jelicic, B. Srbinovski, V. Bilas, E. Popovici, and L. Benini, “Design, Implementation, and Performance Evaluation of a Flexible Low-Latency Nanowatt Wake-Up Radio Receiver,” *IEEE Transactions on Industrial Informatics*, vol. 12, no. 2, pp. 633–644, 2016.
- [3] M. Masoudinejad, J. Emmerich, D. Kossmann, A. Riesner, M. Roidl, and M. ten Hompel, “A measurement platform for photovoltaic performance analysis in environments with ultra-low energy harvesting potential,” *Sustainable Cities and Society*, vol. 25, pp. 74–81, 2015.
- [4] M. Masoudinejad, A. K. Ramachandran Venkatapathy, J. Emmerich, and A. Riesner, “Smart Sensing Devices for Logistics Application,” in *Sensor Systems and Software*, M. Magno, F. Ferrero, and V. Bilas, Eds. Cham: Springer International Publishing, 2017, vol. 205, pp. 41–52, dOI: 10.1007/978-3-319-61563-9_4. [Online]. Available: http://link.springer.com/10.1007/978-3-319-61563-9_4

- [5] M. Roidl, J. Emmerich, A. R. A., M. Masoudinejad, D. Kaulbars, C. Ide, C. Wietfeld, and M. ten Hompel, "Performance Availability Evaluation of Smart Devices in Materials Handling Systems," in *IEEE ICC Workshops on Internet of Things*, 2014, pp. 6–10.
- [6] M. Roidl, J. Emmerich, M. Masoudinejad, A. Riesner, and M. T. Hompel, "Entwicklung eines Versuchsfelds für grosse Systeme intelligenter Behälter," *Logistics Journal*, vol. 2014, 2014.
- [7] R. Falkenberg, M. Masoudinejad, M. Buschhoff, A. K. R. Venkatapathy, D. Friesel, M. t. Hompel, O. Spinczyk, and C. Wietfeld, "PhyNetLab: An IoT-Based Warehouse Testbed," in *IEEE 5th Workshop on Information Technologies for Logistic*. Prague, Czech Republic: IEEE, 2017, arXiv: 1706.09219. [Online]. Available: <http://arxiv.org/abs/1706.09219>
- [8] A. S. Weddell, G. V. Merrett, and B. M. Al-Hashimi, "Photovoltaic sample-and-hold circuit enabling MPPT indoors for low-power systems," *IEEE Transactions on Circuits and Systems I: Regular Papers*, vol. 59, no. 6, pp. 1196–1204, 2012. [Online]. Available: <http://ieeexplore.ieee.org/lpdocs/epic03/wrapper.htm?arnumber=6108371>
- [9] V. Salas, E. Olias, A. Barrado, and A. Lazaro, "Review of the maximum power point tracking algorithms for stand-alone photovoltaic systems," *Solar Energy Materials and Solar Cells*, vol. 90, no. 11, pp. 1555–1578, 2006.
- [10] A. N. A. Ali, M. H. Saied, M. Z. Mostafa, and T. M. Abdel-Moneim, "A survey of maximum PPT techniques of PV systems," in *IEEE Energytech*. IEEE, 2012, pp. 1–17. [Online]. Available: <http://ieeexplore.ieee.org/lpdocs/epic03/wrapper.htm?arnumber=6304652>
- [11] H. J. El-Khozondar, R. J. El-Khozondar, K. Matter, and T. Suntio, "A review study of photovoltaic array maximum power tracking algorithms," *Renewables: Wind, Water, and Solar*, vol. 3, no. 1, pp. 1–8, 2016. [Online]. Available: <http://www.jrenewables.com/content/3/1/3>
- [12] M. Masoudinejad, "A Power Model for DC-DC Boost Converters Operating in PFM Mode," TU Dortmund University, Tech. Rep., 2017. [Online]. Available: http://sfb876.tu-dortmund.de/PublicPublicationFiles/masoudinejad_2017a.pdf
- [13] Texas Instruments, "BQ25505: Ultra Low-Power Boost Charger With Battery Management and Autonomous Power Multiplexer for Primary Battery in Energy Harvester Applications," 2015. [Online]. Available: <http://www.ti.com/lit/ds/symlink/bq25505.pdf>
- [14] T. Instruments, "BQ25570: Ultra Low-Power Boost Charger With Battery Management and Autonomous Power Multiplexer for Primary Battery in Energy Harvester Applications," 2015. [Online]. Available: <http://www.ti.com/lit/ds/symlink/bq25570.pdf>

- [15] M. Masoudinejad, “Energy Harvesting Characteristics under Ultra-Low Light,” *Technical report for Collaborative Research Center SFB 876 Providing Information by Resource-Constrained Data Analysis*, vol. 2016, no. 2016, pp. 41–44, 2016. [Online]. Available: http://sfb876.tu-dortmund.de/PublicPublicationFiles/sfbgk_etal_2016a.pdf
- [16] T. Instruments, “User’s Guide for bq25505 Battery Charger Evaluation Module for Energy Harvesting,” 2014. [Online]. Available: <http://www.ti.com/lit/ug/slueaa8a/slueaa8a.pdf>
- [17] —, “User’s Guide for bq25570 Battery Charger Evaluation Module for Energy Harvesting,” 2014. [Online]. Available: <http://www.ti.com/lit/ug/slueaa7a/slueaa7a.pdf>
- [18] M. Masoudinejad, J. Emmerich, D. Kossmann, A. Riesner, M. Roidl, and M. ten Hompel, “Development of a measurement platform for indoor photovoltaic energy harvesting in materials handling applications,” in *6th International Renewable Energy Congress*, 2015, pp. 1–6.
- [19] Keysight, “Keysight B2961a/B2962a, 6.5 Digit Low Noise Power Source,” 2016. [Online]. Available: <http://literature.cdn.keysight.com/litweb/pdf/5991-0663EN.pdf?id=2257912>
- [20] —, “Keysight B2900a Series Precision Source/Measure Unit,” 2017. [Online]. Available: <http://literature.cdn.keysight.com/litweb/pdf/5990-7009EN.pdf?id=2035016>
- [21] D. Pyle, *Data Preparation for Data Mining*, 1st ed. San Francisco, Calif: Morgan Kaufmann, Apr. 1999.
- [22] K. Singh and S. Upadhyaya, “Outlier detection: applications and techniques,” *International Journal of Computer Science Issues*, vol. 9, no. 1, pp. 307–323, 2012. [Online]. Available: <http://www.datascienceassn.org/sites/default/files/Outlier%20Detection%20-%20Applications%20And%20Techniques.pdf>
- [23] C. C. Aggarwal, *Outlier Analysis*. Springer, Dec. 2016, google-Books-ID: KyG1DQAAQBAJ.
- [24] C. Leys, C. Ley, O. Klein, P. Bernard, and L. Licata, “Detecting outliers: Do not use standard deviation around the mean, use absolute deviation around the median,” *Journal of Experimental Social Psychology*, vol. 49, no. 4, pp. 764–766, Jul. 2013. [Online]. Available: <http://www.sciencedirect.com/science/article/pii/S0022103113000668>

Appendices

A Program

```
%=====
% * This program gets the collected data from the BQ255xx-EVM
    board collected
% * by:
% * Keysight source measurement units models:
% * B2902A Precision Source Measurement Unit
% * OR
% * B2962A Power Source
% *
% * It filters the data,
% * removes the MPPT peaks
% * finds out the data state at each time instant
% * saves the data in a Matrix
%-----
% * <<< COPYRIGHT >>>
% * Code written by: MOJTABA MASOUDINEJAD
% * email: mojtaba.masoudinejad@tu-dortmund.de
%-----
% last modification: 30.03.2017 @ 14:20 in Dortmund
%=====
clear all % clean up the workspace
Origin = '~\BQ70_CP_Raw'; % Folder name of original data
Dest = '~\BQ70_CP_Pro'; % Folder name of destination (storage
)
Dest_Prob = '~\DataProblems'; % Folder name for data with
    error
cd (Origin) % go to raw data folder
Files=dir(fullfile('*.mat')); % get name of all available
    xperiments
%cd ..
for j=1:size(Files,1)
    cd (Origin)
    load(Files(j).name)
    Data =eval(strrep(Files(j).name, '.mat', ''));
    BQ_Type = Files(j).name(3:4); % load data into a local
        param
%-----
V_oc = Data.Config.V_oc;
CH1_Device = Data.Config.CH1_Meas;
CH2_Device = Data.Config.CH2_Meas;
```



```

Date = Data.Config.Date;
Ts = Data.Config.Sample_Time;
MPPT_Perc= Data.Config.MPPT;
if Data.Config.C_In >= 1e-3
    Cur =strcat(num2str(1e3*Data.Config.C_In),'m');
else
    Cur =strcat(num2str(1e6*Data.Config.C_In),'u');
end
if Data.C_In >= 1e-3
    Cur =strcat(num2str(1e3*Data.C_In),'m');
else
    Cur =strcat(num2str(1e6*Data.C_In),'u');
end
Exp_type = 'CP';
Inductor = '22mH';
Msr_Err = 'No measurement error';
T = Data.Raw.Time;
V = Data.Raw.Voltage;
C = [Data.Raw.Current(:,1),-Data.Raw.Current(:,2)];
if V_oc == 0.5
    Voc='05';
else
    Voc=num2str(10*V_oc);
end
In_Curr = [min(C(:,1)),max(C(:,1))];
V_Storage = [min(V(:,2)),max(V(:,2))];
%*****
% Filtering data using moving median
% window should be at least as a MPPT period long at each
% side
% MPPT takes 5 samples -> size =6
Window_Size = 6;
FV = movmedian(V,2*Window_Size+1);
FC = movmedian(C,2*Window_Size+1);
% find the operational stage of the BQ, based on the Vstr
% Logical operational stage
OV_State = (FV(:,2)>=4.19); % overvoltage protection state
CS_State = (FV(:,2)<=1.74); % cold start state
NP_State = bitand(~OV_State,~CS_State);% normal operation
state
% numerical operational stage
OP_Stage = T*0;
% condition values:
% 0: Over voltage protection
% 1: Normal Operation
% 2: Cold start

```

```

for i=1:size(OP_Stage,1)
    if OV_State(i)
        OP_Stage(i) = 0;
    elseif NP_State(i)
        OP_Stage(i) = 1;
    elseif CS_State(i)
        OP_Stage(i) = 2;
    end
end
% finding MPPT
% normalizes the data to avoid amplitude dependency
Diff_V = abs(V(:,1)-FV(:,1));
MPPT_Running = false(size(T));
% MPPT happens only during the NP_State
% MPPT is the outlier of a median with 15 second window
% from each side
% overall median window size = 30 sec. (MPPT happens
% every 16 sec.!)
MPPT_Running(any(NP_State,2)) = isoutlier(Diff_V(any(
    NP_State,2)), 'movmean', 30*(1/Ts));
% checking if a MPPT is missed
[rId, cId] = find(MPPT_Running) ;
srId=[rId(1,1);rId(1:end-1,1)]; % shifting indexes to
% find the distance
if max(rId-srId)>16.5*(1/Ts) % if two subsequent MPPT are
% further than 16.5 sec.
    MPPT_Err = 'MPPT missed';
    Err_stat1 = true;
    disp(MPPT_Err) % showing type of error
    Err = Files(j).name % no semicolon to see the error
    % on the workspace
else
    MPPT_Err = 'No MPPT detection error';
    Err_stat1 = false;
end
% finding starting/end point of MPPT periods
Shifted_MPPT = MPPT_Running;
Shifted_MPPT(2:end) = MPPT_Running(1:end-1); % shift data
% 1-bit
MPPT_Start = bitand(MPPT_Running,~Shifted_MPPT); %
% detecting rising edge
MPPT_End = bitand(~MPPT_Running,Shifted_MPPT); % detecting
% falling edge
% finding the step changes in the V_str
Vstr_Diff=[abs(diff(FV(:,2)));0]; % finding the
% derivation

```

```

V_Str_Changing=(Vstr_Diff>0.02); % finding the outliers
    in the derivation
% finding starting/end point of the storage voltage
    change
Shifted_V_Str_Changing = V_Str_Changing;
Shifted_V_Str_Changing(2:end) = V_Str_Changing(1:end-1);
    % shift data 1-bit
Vstr_Change_Start = bitand(V_Str_Changing,~
    Shifted_V_Str_Changing); % detecting rising edge
Vstr_Change_End = bitand(~V_Str_Changing,
    Shifted_V_Str_Changing);% detecting falling edge
% Finding and storing the system condition
% Building logical vector to define the system state
Normal_Running = false(size(T));
MM_Running = false(size(T));
Unstable_Running = false(size(T));
Cond_Index= [1,1,3];
j=1; %initialize labeling number
stat=T*0+3; % numerical state
% condition values:
% 0: MPPT running
% 1: Normal Operation
% 2: Storage voltage is changing, invalid data (
    unstable)
% 3: Storage voltage has changed, system is operating
    non-optimal till the next MPPT measurement
for i=2:size(T,1)
    if MPPT_Start(i)
        Cond_Index=[Cond_Index;i,0,0];
        Cond_Index(j,2)=i-1;
        j=j+1;
        stat(i)=0;
    elseif MPPT_End(i)
        Cond_Index=[Cond_Index;i,0,1];
        Cond_Index(j,2)=i-1;
        j=j+1;
        stat(i)=1;
    elseif Vstr_Change_Start(i)
        Cond_Index=[Cond_Index;i,0,2];
        Cond_Index(j,2)=i-1;
        j=j+1;
        stat(i)=2;
    elseif Vstr_Change_End(i)
        Cond_Index=[Cond_Index;i,0,3];
        Cond_Index(j,2)=i-1;
        j=j+1;

```

```

        stat(i)=3;
    else
        stat(i)=stat(i-1);
    end
    % Storing the state into the related logical vector
    if stat(i)==1 % MPPT state is already stored
        Normal_Running(i) = true;
    elseif stat(i)==2
        Unstable_Running(i) = true;
    elseif stat(i)==3
        MM_Running(i) = true;
    end
end
% Preparing finishing value of the last row
Cond_Index(end,2)=i;
% finding if a state is repeated
Cond_diff=diff(Cond_Index(:,3));
if any(Cond_diff(:,1)==0)
    Condition_Err = 'State mislabel';
    Err_stat2 = true;
    disp(Condition_Err) % showing type of error
    Err = Files(j).name % no semicolon to see the error
                        on the workspace
else
    Condition_Err = 'No mislabeling error';
    Err_stat2 = false;
end
% making the averaging
V_Avg = zeros(size(Cond_Index,1),2);
C_Avg = zeros(size(Cond_Index,1),2);
for i=1:size(Cond_Index,1)
    V_Avg(i,:) = mean(V(Cond_Index(i,1):Cond_Index(i,2)
        ,:));
    C_Avg(i,:) = mean(C(Cond_Index(i,1):Cond_Index(i,2)
        ,:));
end
Voc_real=zeros(size(Cond_Index,1),1)+V_oc;
Voc_operational=zeros(size(Cond_Index,1),2);
Voc_operational(2:end,1)= V_Avg(1:end-1,1);
Voc_operational(1,1) = V_Avg(1,1);
Voc_operational(3:end,2)= V_Avg(1:end-2,1);
Voc_operational(1:2,2) = V_Avg(1:2,1);
Sys_Data= [Cond_Index,V_Avg,C_Avg,Voc_real,
    Voc_operational];
MPPT_stages = Sys_Data(any(Sys_Data(:,3)==0,2),:);
MPPT_stages = MPPT_stages(:,4:8);

```

```

Normal_stages = Sys_Data(any(Sys_Data(:,3)==1,2),:);
NS_Duration = Normal_stages(:,2)-Normal_stages(:,1); %
    duration of normal state
NS_Short=any(NS_Duration<2*(1/Ts),2); % is duration
    shorter than 2 sec?
Normal_stages(any(NS_Short,2),:)=[]; % remove too short
    normal data
Normal_stages = [Normal_stages(:,4:9),100*Normal_stages
    (:,4)./Normal_stages(:,9)];
MM_stages = Sys_Data(any(Sys_Data(:,3)==3,2),:);
MM_stages = MM_stages(:,4:10);
%*****
% building the structure
State_Info = '[state 1st index, state last index, Label
    No., Vin, Vout, Cin, Cout]';
Outcome_Info = ['MPPT: [Vin, Vout, Cin, Cout, Voc];
    Normal: [Vin, Vout, Cin, Cout, Voc, Voc from last MPPT
    , Percentage]; Mismatch: [Vin, Vout, Cin, Cout, Voc,
    Voc from last Normal operation, Voc from last MPPT]'];
Condition_Info = '0: Over voltage protection;    1: Normal
    Operation;    2: Cold start';
Label_Info = '0: MPPT running;    1: Normal Operation;
    2: Storage voltage is changing, invalid data (unstable
    );    3: Storage voltage has changed, system is
    operating non-optimal till the next MPPT measurement';
BQ.Config = struct('Date',Date,'BQ_Type',strcat('255',
    BQ_Type),'MPPT',MPPT_Perc,'L',Inductor);
BQ.Experiment = struct('Type',Exp_type,'I_pv',Cur,'V_oc',
    V_oc,'Sample_Time',Ts,'In_Ch',CH1_Device,'Out_Ch',
    CH2_Device,'In_Curr',In_Curr,'V_Storage',V_Storage);
BQ.Time = Data.Raw.Time;
BQ.Raw = struct('Voltage',V, 'Current',C);
BQ.Filter = struct('Voltage',FV, 'Current',FC);
BQ.State = struct('Condition',[], 'Label',[]);
BQ.State.Condition = struct('Numerical',OP_Stage,'Info',
    Condition_Info,'Over_Volt',OV_State, 'Normal',NP_State
    , 'Cold_Start',CS_State);
BQ.State.Label = struct('Numerical',stat,'Info',
    Label_Info,'MPPT',MPPT_Running, 'Normal',
    Normal_Running, 'Mismatch',MM_Running);
BQ.Classified = struct('Data',Sys_Data(:,1:7), 'Info' ,
    State_Info);
BQ.Outcome = struct('Info', Outcome_Info, 'MPPT',
    MPPT_stages, 'Normal',Normal_stages, 'Mismatch',
    MM_stages);
BQ.Errors = struct('Measurement', Msr_Err, 'MPPT',

```

```

        MPPT_Err, 'Labeling', Condition_Err);
%-----
% saving the structure
% defining the name
add = strcat('BQ', BQ_Type, '_', Exp_type, '_', Voc, '_', Cur);
assignin('base', add, BQ);
filename = strcat(add, '.mat'); % building the mat name
    for the data
if ~Err_stat1 && ~Err_stat2
    cd (Dest)
    save(filename, add)
else
    cd (Dest_Prob)
    save(filename, add)
end
end
clear all

```

B Data sheets

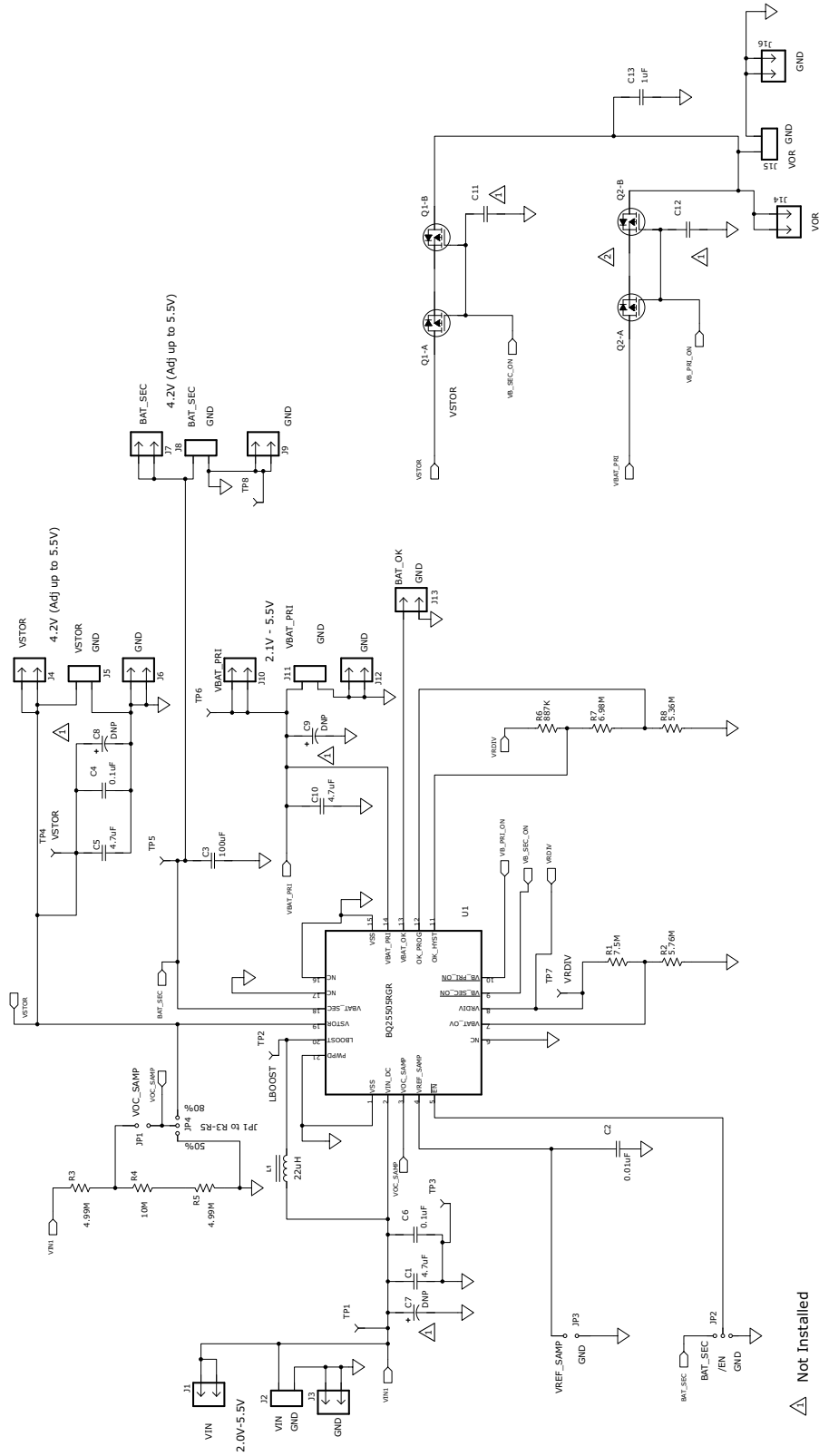
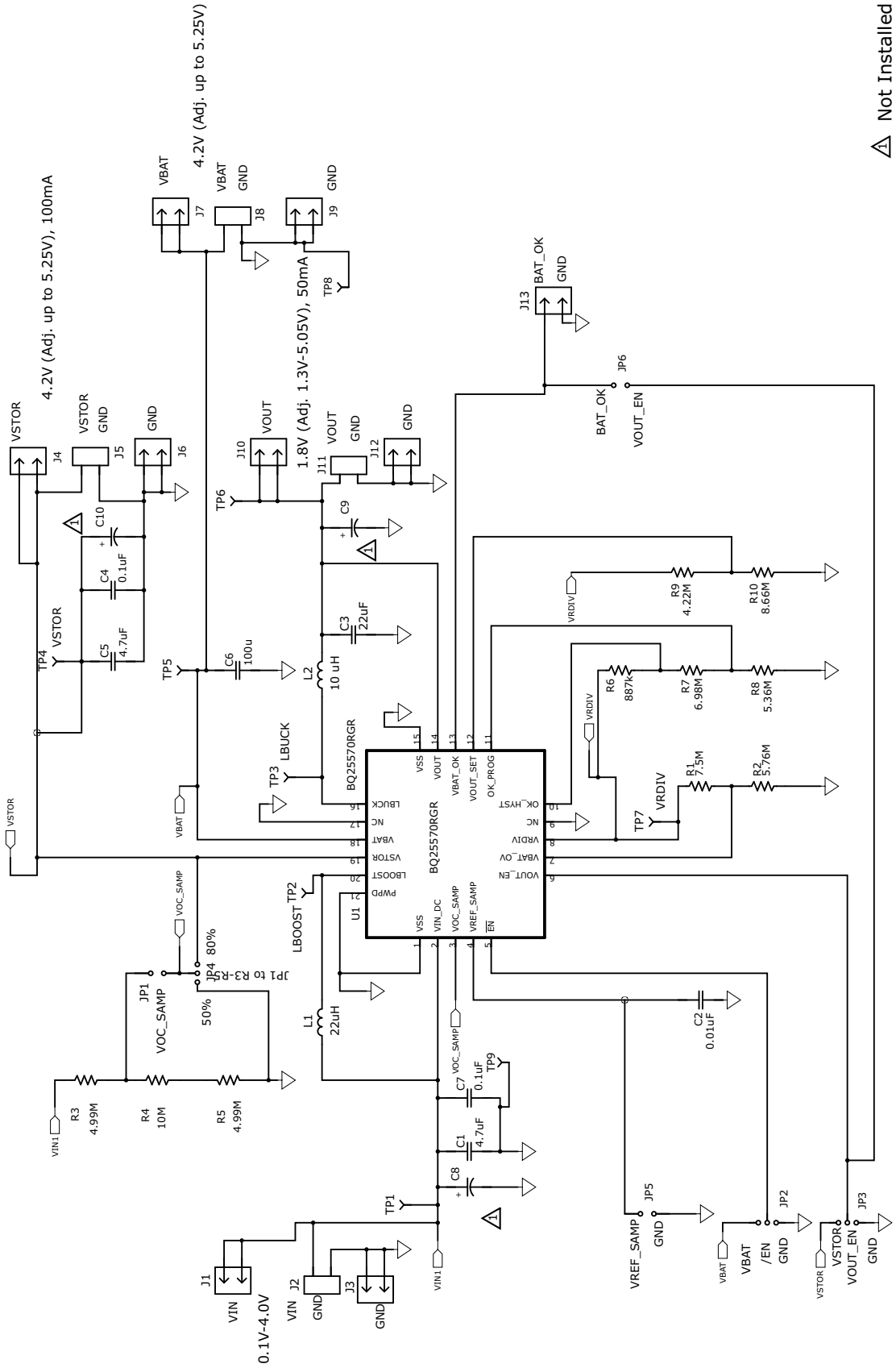


Figure A.1: Schematic representation of the BQ25505-EVM evaluation board [16]



⚠ Not Installed

Figure A.2: Schematic representation of the BQ25570-EVM evaluation board [17]